JOURNAL OF AGRICULTURAL AND FOOD CHEMISTRY

Article

pubs.acs.org/JAFC

Characteristics of Activated Carbon and Carbon Nanotubes as Adsorbents To Remove Annatto (Norbixin) in Cheese Whey

Yue Zhang, Kang Pan, and Qixin Zhong*

Department of Food Science and Technology, University of Tennessee in Knoxville, Knoxville, Tennessee 37996, United States

ABSTRACT: Removing annatto from cheese whey without bleaching has potential to improve whey protein quality. In this work, the potential of two activated carbon products and multiwalled carbon nanotubes (CNT) was studied for extracting annatto (norbixin) in aqueous solutions. Batch adsorption experiments were studied for the effects of solution pH, adsorbent mass, contact duration, and ionic strength. The equilibrium adsorption data were observed to fit both Langmuir and Freundlich isotherm models. The thermodynamic parameters estimated from adsorption isotherms demonstrated that the adsorption of norbixin on three adsorbents is exothermic, and the entropic contribution differs with adsorbent structure. The adsorption kinetics, with CNT showing a higher rate than activated carbon, followed the pseudo first order and second order rate expressions and demonstrated the significance of intraparticle diffusion. Electrostatic interactions were observed to be significant in the adsorption. The established adsorption parameters may be used in the dairy industry to decolorize cheese whey without applying bleaching agents.

KEYWORDS: *activated carbon, carbon nanotubes, norbixin (annatto) removal, isotherm models, kinetics models, electrostatic interactions*

INTRODUCTION

Norbixin (Scheme 1), known as annatto, is used to produce colored cheeses, with most being contained in cheese curd and the rest ending up in cheese whey. With the established functional and nutritional qualities of whey proteins, manufacturing whey protein ingredients is a significant sector in the dairy industry nowadays. The increasing demand for whey proteins calls for the utilization of whey originating from the production of both colored and uncolored cheeses. To utilize colored cheese whey, a bleaching process is employed to decolorize liquid whey prior to other unit operations. Hydrogen peroxide and benzoyl peroxide are bleaching agents that oxidize norbixin and possibly also proteins, which can deteriorate sensory and functional qualities of whey protein products.[1] Removing fat globules was observed to significantly reduce the color of whey protein concentrate but caused the loss of some proteins.[2] Enzymatic bleaching has also been studied but may still have the issue of flavor defects resulting from bleaching.[3] Furthermore, our previous work demonstrated that norbixin has strong binding affinity to whey proteins.[4] Therefore, physical methods may be desired, e.g., adsorbents that are effective in removing annatto at whey production conditions.

Scheme 1. The Molecular Structure of Norbixin

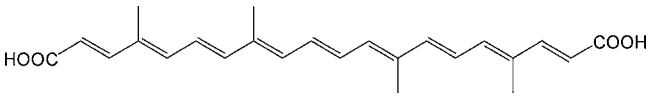

In the present study, conventional adsorbents, two types of activated carbon, and multiwalled carbon nanotubes (CNT) were studied for their potential to remove annatto in aqueous solutions. Activated carbon products have porous structures and large internal surface areas available for adsorption and are popular choices for various treatments.[5] The powdered activated carbon is widely used in drinking water and wastewater treatments to remove organic compounds.[6] Activated carbon is also used as a processing aid to decolorize clarified apple juice and alcoholic beverages such as beer and wine in the food industry.[7] In a recent study, activated carbon was observed to effectively decolorize Japanese soy sauce and maintain sensory quality better than activated clay, diatomaceous earth, and magnesium oxide.[8] As for CNT, several studies have demonstrated its potential as processing aids in food manufacturing. As a promising group of nanomaterials purifying drinking water,[9] CNT have been proved as effective adsorbents of both chemical and biological contaminants such as heavy metals, polycyclic aromatic compounds, bacteria and viruses.[10,11] Additionally, CNT can remove free radicals,[12] which may further minimize the undesired oxidation reactions in cheese whey during whey protein recovery and subsequent storage and applications.

To evaluate the potential of activated carbons and multiwalled CNT in cheese whey processing, the effectiveness of adsorbents in removing norbixin was studied for solution chemistry, temperature, and adsorbent level. The equilibrium and kinetic adsorption data were analyzed using various models to understand the characteristics of adsorption. Where appropriate, the data were correlated to physicochemical properties of adsorbents such as surface area, pore size, and surface charge.

Received: June 9, 2013
Revised: August 23, 2013
Accepted: August 27, 2013
Published: August 27, 2013

dx.doi.org/10.1021/jf402537y | *J. Agric. Food Chem.* 2013, 61, 9230−9240

MATERIALS AND METHODS

Materials. Activated carbon SGL 8 × 30 (CA) and CAL 12 × 40 (CB) were from Calgon Carbon Corp. (Pittsburgh, PA). The multiwalled CNT was from CNano Technology Ltd. (Santa Clara, CA). The three carbon agents were washed several times with distilled water and dried in an oven at 150 °C for 24 h before use. Annatto WS28 containing 2.8% norbixin was a liquid product from DDWilliamson, LLC (Port Washington, WI). Whey protein isolate (WPI) was a product from Hilmar Ingredients (Hilmar, CA). All other chemicals used in this study were obtained from either Sigma-Aldrich Corp. (St. Louis, MO) or Fisher Scientific (Pittsburgh, PA).

Characterization of Structures of Adsorbents. Surface area and pore size of three adsorbents were determined by Micromeritics Analytical Services (Norcross, GA) using the nitrogen adsorption isotherm method at 77 K on a Micromeritics Tristar II 3020 analyzer. Parameters for porous media like the Brunauer−Emmett−Teller (BET) surface area, micropore area, external area, total pore volume and micropore volume were measured and were derived using the *t*-plot method. The micrographs of adsorbents were imaged using a LEO 1525 surface scanning electron microscope (LEO Electron Microscopy, Oberkochen, Germany).

Characterization of Surface Charge Properties of Adsorbents. The point of zero charge (PZC) method[13] was used to characterize surface charge properties of the three adsorbents. Vials were filled with 15 mL of a 0.5 N NaCl aqueous solution, added with different amounts of adsorbents, and adjusted to pH 5.7 or 11.1 using 1 N HCl or NaOH. The vials were then incubated at 25 °C in a C76 shaking water bath (New Brunswick Scientific, Edison, NJ) operating at 130 rpm. The equilibrium pH of suspensions was measured after 24 h to determine the pH corresponding to PZC (pH_{PZC}).

Adsorption Properties. Adsorption studies were carried out in triplicate by mixing various amounts of the adsorbent with aqueous solutions containing 500 ppm norbixin,[14] unless noted otherwise. After incubation for preselected conditions detailed below in the above shaking water bath, the mixture was centrifuged at 6,700*g* for 5 min using an Eppendorf MiniSpin plus centrifuge (Hamburg, Germany), and 100 μL of the supernatant was transferred and diluted to 3 mL with distilled water for determination of norbixin concentration by measuring the absorbance at 460 nm (Abs_{460})[15] using a UV−vis spectrophotometer (model 201, Thermo Scientific, Waltham, MA). Preliminary experiments showed a linear correlation between Abs_{460} (in the range of 0−1.8) and norbixin concentration (0−12 ppm). The removal efficiency was calculated as follows:

$$\text{removal}\ (\%) = \left(\frac{C_0 - C}{C_0}\right) \times 100\% \tag{1}$$

where C_0 is the initial concentration, and C is the residual concentration of norbixin after treatment at a specific combination of adsorption conditions.

Effects of pH on Norbixin Adsorption. The concentration of CA, CB, and CNT was 16, 16, and 1.6 g/L, respectively. The suspensions were adjusted to pH 2.5−10.5 using 1 N HCl or NaOH and were mixed using an end-to-end shaker (Lab Industries Inc., Berkeley, CA) at room temperature (23 °C) for 2 h.

Effects of Adsorbent Mass. The effects of adsorbent dose on the adsorption of norbixin were studied at pH 6.4 and 23 °C. The adsorption duration was 2 h.

Adsorption Isotherms. To establish adsorption isotherms, each adsorbent was mixed in amber vials with 10 mL of aqueous solution with a norbixin concentration from 50 to 500 ppm. The amber vials were used to minimize norbixin degradation during incubation. The concentration of CA, CB, and CNT was 64, 64, and 6.4 g/L, respectively. The samples were adjusted to pH 6.4 and were incubated for 24 h in the above shaking water bath operating at three temperatures (298, 313, and 328 K). After centrifugation and determination of the remaining norbixin as above, the amount of norbixin adsorbed at equilibrium onto unit mass of carbon agent, q_e (mg g^{-1}), was considered as the adsorption capacity that was calculated using the following equation:

$$q_e = (C_0 - C_e)\frac{V}{W} \tag{2}$$

where C_e is the equilibrium concentration of norbixin (mg/L), W is the mass of adsorbent (g), and V is the volume of the solution (L).

Langmuir and Freundlich models were used to analyze adsorption isotherm data. The Langmuir isotherm equation (eq 3) assumes a surface with homogeneous binding sites, equivalent sorption energies and no transmigration of adsorbate on the surface.[16] The Freundlich isotherm is an empirical equation based on an exponential distribution of adsorption sites and energies, with the mathematical form in eq 4.[16]

$$\frac{C_e}{q_e} = \frac{C_e}{q_{max}} + \frac{1}{q_{max}k_L} \tag{3}$$

where q_{max} and k_L represent the maximum adsorption capacity and the adsorption equilibrium constant (L/mg) related to the apparent energy of sorption. A plot of C_e/q_e versus C_e gives a straight line with a slope of $1/q_{max}$ and an intercept of $1/(q_{max}k_L)$.[16]

$$\ln q_e = \ln k_F + \frac{1}{n}\ln C_e \tag{4}$$

where k_F (mg/g) and n are the Freundlich constants related to the adsorption capacity and adsorption intensity, respectively.[16] The values of k_F and n can be calculated from the slope and intercept of the plot, respectively.

Adsorption Kinetics. Each adsorbent was mixed in amber vials with the 500 ppm norbixin solution and adjusted to pH 6.4. The vials were incubated at 25 °C in the above shaking water bath. One milliliter samples were collected from the vials after 0, 1, 2, 3, 4, 5, 6, 7.5, and 9 h for CA and CB, while the sampling times were 0, 30, 50, 70, 90, 120, 150, 210, 270, 340, and 540 min for CNT.

The kinetics of norbixin adsorption onto absorbents was analyzed using pseudo first order,[17] pseudo second order,[17] Elovich,[18] and intraparticle diffusion[19,20] kinetic models in eqs 5, 6 and 7, 8, and 9, respectively.

$$\log(q_e - q_t) = \log q_e - \frac{k_1}{2.303}t \tag{5}$$

where q_t is the amount of norbixin adsorbed on adsorbent (mg g^{-1}) at time point t, and k_1 is the rate constant of adsorption (h^{-1}). If the plot of $\log(q_e - q_t)$ against t gives a linear relationship, constants k_1 and q_e can be determined from the slope and intercept of linear regression, respectively.

$$\frac{t}{q_t} = \frac{1}{k_2 q_e^{\,2}} + \frac{1}{q_e}t \tag{6}$$

where k_2 is the second order rate constant of adsorption (g mg^{-1} h^{-1}). The magnitudes of q_e and k_2 are determined from the slope and intercept of the plot of t/q_t against t, and the initial adsorption rate h can be calculated by the following equation:[21]

$$h = k_2 q_e^{\,2} \tag{7}$$

$$q_t = \frac{1}{\beta}\ln \alpha\beta + \frac{1}{\beta}\ln t \tag{8}$$

where α is the initial adsorption rate (mg g^{-1} h^{-1}) and β is the desorption constant (g mg^{-1}). If norbixin adsorption on carbon agents fits the model, a plot of q_t versus ln t should yield a linear relationship with a slope of $(1/\beta)$ and an intercept of $(1/\beta)$ ln $(\alpha\beta)$. The values of α and β can then be determined from the slope and intercept after linear regression.

$$q_t = K_{dif}t^{1/2} + I \tag{9}$$

where I (mg g^{-1}) is the intercept and K_{dif} is the intraparticle diffusion rate constant (mg g^{-1} $min^{-1/2}$). The value of q_t is linearly correlated with $t^{1/2}$, and the K_{dif} can be evaluated directly from the slope of the plot.

dx.doi.org/10.1021/jf402537y | J. Agric. Food Chem. 2013, 61, 9230−9240

Adsorption of WPI on Adsorbents. The adsorption of WPI on adsorbents was investigated at various pH conditions at room temperature (23 °C). CA, CB, and CNT were suspended at 16, 16, and 1.6 g/L, respectively, in 0.2% WPI solutions, and the mixtures were adjusted to pH 2.5−10.5 using 1 N HCl or NaOH. After mixing using an end-to-end shaker (Lab Industries Inc., Berkeley, CA) at room temperature (23 °C) for 2 h and centrifugation as above, the concentration of WPI in the supernatant was determined by the bicinchoninic acid (BCA) method using an incubation temperature of 37 °C for 30 min. The absorbance at 562 nm was measured using a UV−vis spectrophotometer (model 201, Thermo Scientific, Waltham, MA). Bovine serum albumin was used as a reference.

Statistical Analysis. The kinetics model discrimination test was performed using MatLab (Version 2013a, The MathWorks, Inc., Natick, MA). The Akaike Information Criterion (AIC), which compares the information captured by models, was calculated by using eq 10.[22] The model with the lowest AIC was treated as the best fit, if there were no other criteria for specific models.

$$\mathrm{AIC} = n\ln(2\pi) + n\ln\left(\frac{\mathrm{SSE}}{n}\right) + n + 2(\chi + 1) \quad (10)$$

where n is the number of data points, SSE is the error sum of squares, and χ is the number of parameters estimated.

RESULTS AND DISCUSSION

Characteristics of Adsorbents. According to the manufacturer, the CNT have an average diameter of 11 nm and a length of 10 μm. The particle diameter is 0.80−1.00 mm for CA and 0.55−0.75 mm for CB, respectively. Other physical properties were measured and are presented in Table 1.

Table 1. The Pore Size and Surface Area Parameters of Three Adsorbents

property	CA	CB	CNT
BET surface area (m^2/g)	1016.1	1162.7	176.8
t-plot micropore area (m^2/g)	941.1	1074.5	27.5
t-plot external surface area (m^2/g)	75.0	88.2	149.4
BJH adsorption cumulative surface area (m^2/g)	453.0	427.6	193.2
total volume of pores (cm^3/g)	0.57	0.66	0.728
t-plot micropore vol (cm^3/g)	0.42	0.48	0.021
BJH adsorption cumulative vol (cm^3/g)	0.35	0.36	0.74
total microporosity ratio	1.36	1.38	34.67
adsorption av pore width (4V/A by BET) (Å)	22.7	22.7	166.2
BJH adsorption av pore width (Å)	31.1	33.7	153.9

Additionally, the ratio of total pore volume to *t*-plot micropore volume was calculated to be the total microporosity ratio to evaluate the degree of porosity.[23] The total microporosity ratio of 34.67 for CNT suggests that the CNT have mostly mesopores and macropores, while the much smaller values of CA (1.36) and CB (1.38) indicate their microporous structures.[24] Both CA and CB had a porous structure with some macropores and mesopores based on SEM (Figures 1A and 1B), indicating relatively high surface areas that agree with the BET surface area in Table 1,[25] with the surface of CA being smoother than that of CB. Activated carbon had a BET surface area several fold higher than CNT (Table 1) that appeared as loose and intertwined tubular structures (Figure 1C).

Additionally, pH_{PZC} was quantified because it indicates net surface charge properties of carbon adsorbents in aqueous media:[16] net positive at pH below pH_{PZC} and net negative at pH above pH_{PZC} .[26] The titration results for three adsorbents

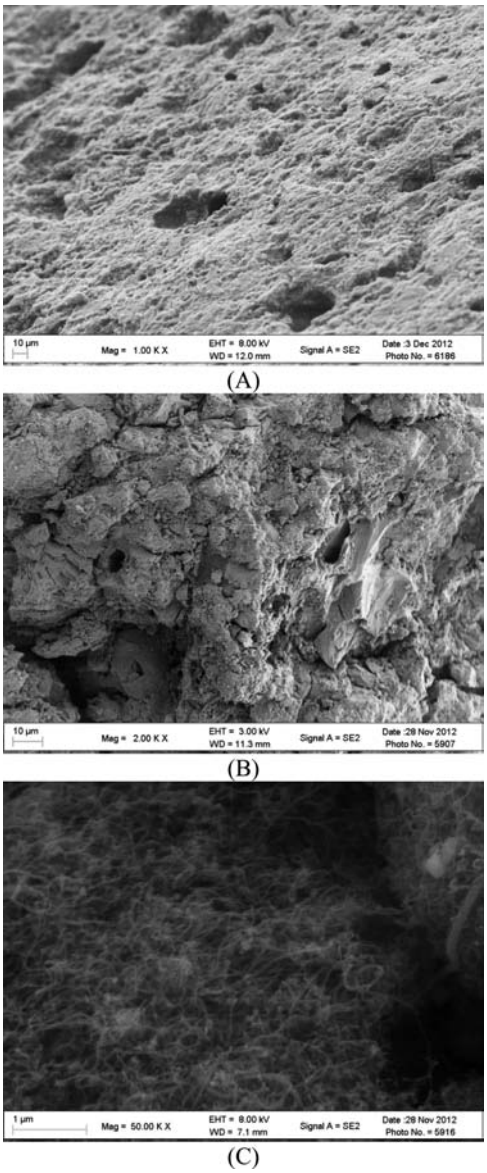

Figure 1. SEM images of CA (A), CB (B), and CNT (C).

are shown in Figure 2, and the pH_{PZC} of CA, CB, and CNT was determined to be 10.8, 10.3, and 8.4, respectively.

Effects of System pH on Norbixin and Whey Protein Adsorption. pH is an important factor of adsorption because it impacts surface charge properties of both adsorbent and adsorbate.[27] Figure 3A shows the influence of pH on norbixin removal. The removal efficiencies of all adsorbents decreased with increasing pH in the pH range from 2.5 to 4.5. The higher removal efficiency and bigger deviations in replications at lower pH can be attributed to the precipitation of annatto at acidic conditions.[28] For CA and CB, the adsorption capacity increased significantly as the pH increased from 4.5 to 10.5. At pH 6.4 and above, norbixin was removed to a greater extent by CB than CA after two hours incubation, which agrees with the larger BET surface area of CB (Table 1). In contrast, the maximum removal efficiency for the case of CNT was observed at pH 6.5, which implies that increasing pH from 6.5 to 10.5 results in the increased repulsion between CNT surface and norbixin.

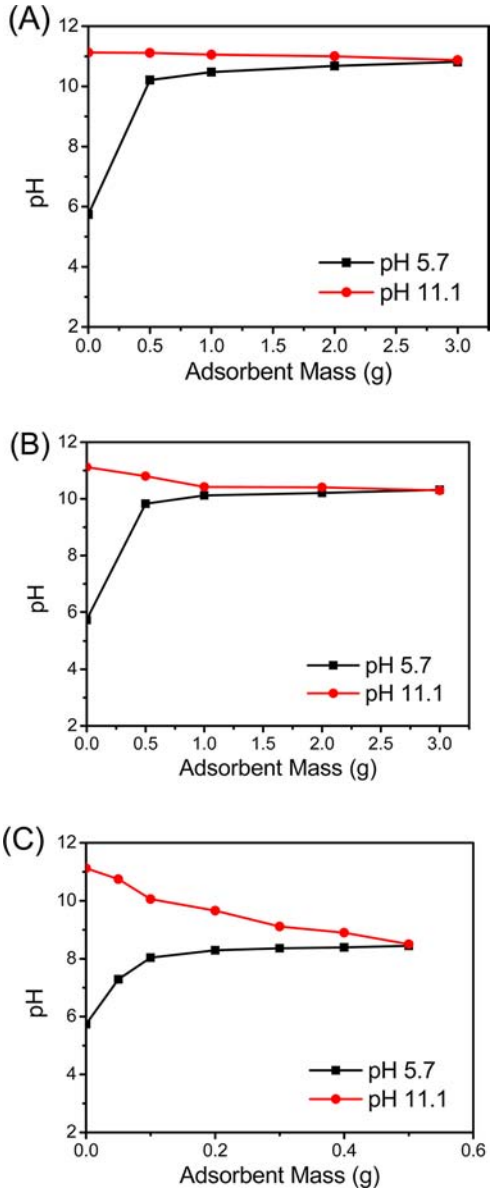

Figure 2. The pH of suspensions with different amounts of CA (A), CB (B), and CNT (C) after 24 h incubation at 298 K. Suspensions were prepared with different amounts of adsorbents suspended in 15 mL of 0.5 N NaCl and adjusted to pH 5.7 or 11.1 before incubation. The pH at the crossover of the acidic and basic curves is referred to as the pH corresponding to the point of zero charge (pH_{PZC}).

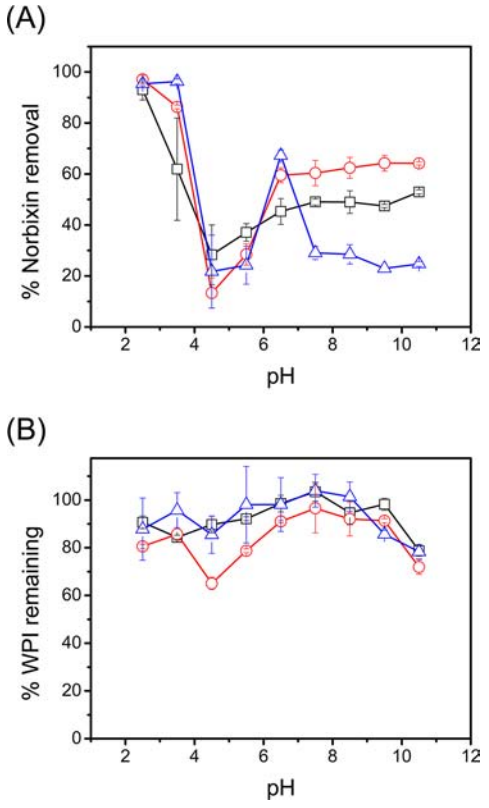

Figure 3. pH effects on norbixin (A) and WPI (B) removal by CA (black squares), CB (red circles), and CNT (blue triangles). Suspensions were prepared with CA, CB, and CNT at a level of 16, 16, and 1.6 g/L, respectively, and 500 ppm annatto (A) or 0.2% w/v WPI (B), adjusted to pH 2.0−10.5, and incubated at 23 °C for 2 h before centrifugation for analysis. Error bars represent the range of duplicate samples.

A practical adsorbent shall be effective in removing norbixin and retaining most proteins. The pH effects on WPI adsorbing on the adsorbents are shown in Figure 3B. Many treatments showed retention of more than 90% protein. At pH of cheese whey (6.4),[29] all three adsorbents had high protein retention. Since all three absorbents have high norbixin removal capacity, especially for CNT (Figure 3A), and good protein retention (Figure 3B) at this pH, no pH adjustment is required when these adsorbents are used to remove annatto from colored cheese whey. The rest of this study was then focused on pH 6.4 only.

Effects of Adsorbent Mass on Norbixin Removal. The adsorption of 500 ppm annatto on different doses of adsorbents at pH 6.4 for 2 h is shown in Figure 4. As the dose of adsorbents increased, the norbixin removal increased significantly for all three adsorbents. It can be attributed to the increased absorbent surface area and adsorption sites.[20]

Isotherm Data Analysis. Like other carotenoids, norbixin is an unstable colorant and factors such as temperature, pH, and oxygen can promote the degradation.[28] As shown in Figure 5, about 57% of norbixin remained after 24 h incubation at ambient conditions. In order to calculate the percentage of norbixin removal by adsorbents accurately, the following adsorption studies were performed in amber vials to minimize the degradation of norbixin. Degradation of norbixin in amber vials was also observed and was used to calibrate the data in the rest of this paper.

In order to optimize the removal conditions, it is important to establish adsorption isotherms for each adsorbent.[30] Langmuir and Freundlich isotherms are the two most common models that can also be used to understand sorption mechanisms, surface properties of adsorbents, and affinities between adsorbates and adsorbents.

Figure 6 presents the adsorption isotherm examples at pH 6.4 and 298 K to reveal the relationship between the norbixin mass adsorbed on unit mass of adsorbent (q_e) and the equilibrium concentration of norbixin (C_e). Table 2 summarizes the parameters in the Langmuir and Freundlich isotherm models at three studied temperatures. The R^2 values exceeding 0.9 and the small SD values suggest that both models fit the experimental results well. The $1/n$ values in the Freundlich model are lower than 1.0 for three adsorbents, indicating that

dx.doi.org/10.1021/jf402537y | J. Agric. Food Chem. 2013, 61, 9230−9240

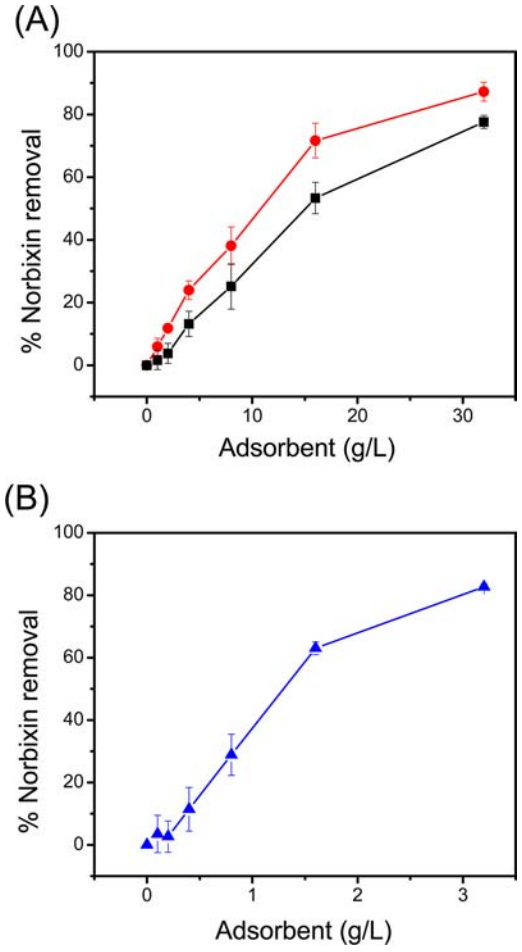

Figure 4. Percentages of norbixin removal after incubating (A) 0–32 g/L CA (black squares) or CB (red circles), or (B) 0–3.2 g/L CNT with 500 ppm norbixin at pH 6.4 and 298 K for 2 h. Error bars represent the range of duplicate samples.

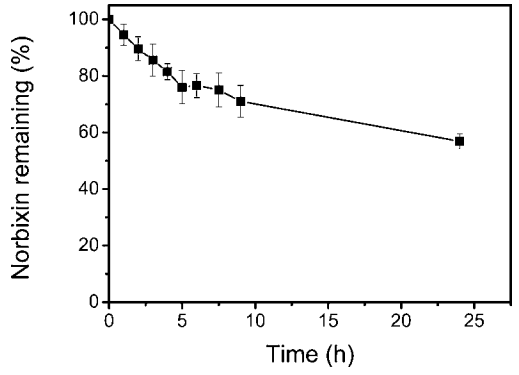

Figure 5. The degradation of norbixin in aqueous solutions at pH 6.4 and ambient conditions (23 °C). Error bars represent the range of duplicate samples.

norbixin adsorbs favorably on all three adsorbents at the studied conditions.[20] The decrease of k_L and k_F with an increase in temperature implies the weakened binding affinity. Conversely, the q_{max} and n did not show an obvious trend of the temperature impact.

Kinetics of Norbixin Adsorption. Figure 7 shows the kinetics of norbixin removal by three adsorbents. The rate of norbixin removal decreased over time, which is expected due to

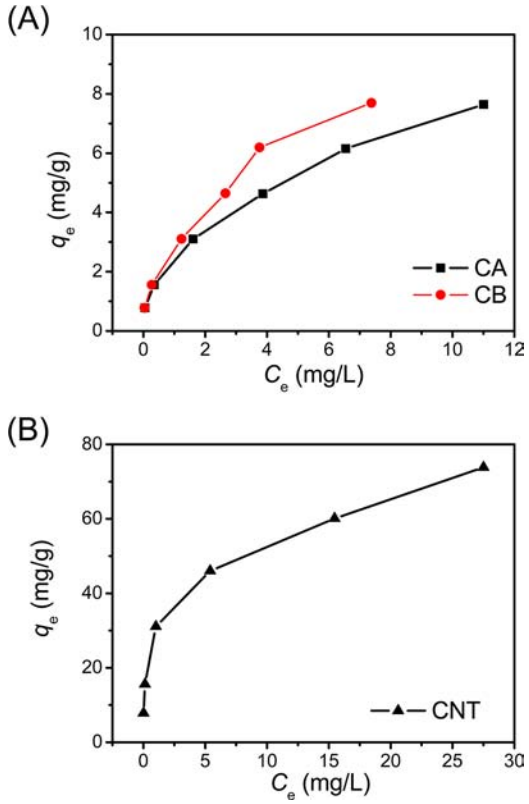

Figure 6. Adsorption isotherms of norbixin on (A) 64 g/L CA or CB and (B) 6.4 g/L CNT at 298 K and pH 6.4.

the reduced availability of adsorption sites and the initial adsorption on external surface of the adsorbent particles proceeded by diffusion of norbixin molecules onto interior adsorption sites. The equilibrium was about 9 h for activated carbons at a high concentration, e.g., 64 g/L, while the adsorption by CNT reached equilibrium in a much shorter time at a high dose, e.g., in 3 h at the 32 g/L dose.

In order to find out the potential rate-controlling steps involved in the adsorption process, the data were fit to four models according to eqs 5–9, plotted in Figure 8 for the example of CA. After fitting the data to models, the obtained parameters in each model and the goodness-of-fit in terms of coefficient of determination (R^2) and AIC values are summarized in Table 3. The adsorption can be described by both pseudo first order and second order equations in most circumstances. The parameters from the pseudo first order model corresponded to the lowest AIC for CA and CB, which agrees with the dominance of the pseudo first order mechanism in adsorption studies.[31] For CNT, the first order equation fits the data better at lower concentrations of CNT, but the value of q_e was underestimated at higher concentrations of CNT, with R^2 values significantly lower than 1. If the q_e estimated from the intercept (eq 5) does not match the experimentally determined q_e, the first order model can not be applied, despite high R^2.[32] Rudzinski et al.[33] suggested that the pseudo first order model is more applicable for the adsorption with longer adsorption times, which is demonstrated by our data. For CNT used at 16 and 32 g/L, the adsorption reached the equilibrium quickly, and the data fit the pseudo second order model well, with the q_e values estimated from the model being consistent with the experimental data.

dx.doi.org/10.1021/jf402537y | J. Agric. Food Chem. 2013, 61, 9230–9240

Table 2. Isotherm Parameters Obtained Using Langmuir and Freundlich Models for Norbixin Adsorbing onto Three Adsorbents at Three Temperatures

		Langmuir				Freundlich			
model	temp (K)	q_{max}(mg/g)	k_L(L/mg)	R^2	SD	n	k_F (mg/g)	R^2	SD
CA	298	8.33	0.39	0.933	0.014	2.32	2.29	0.996	0.012
	313	8.06	0.29	0.932	0.017	3.13	1.98	0.971	0.027
	328	7.09	0.14	0.972	0.008	3.09	1.50	0.950	0.043
CB	298	8.69	0.51	0.917	0.015	2.22	2.67	0.990	0.021
	313	8.40	0.18	0.964	0.010	2.00	1.47	0.996	0.015
	328	9.52	0.12	0.939	0.012	1.67	1.16	0.996	0.017
CNT	298	71.94	0.53	0.977	0.001	3.45	25.71	0.996	0.008
	313	74.07	0.19	0.983	0.001	2.50	15.33	0.992	0.016
	328	66.67	0.18	0.977	0.001	2.95	15.64	0.985	0.019

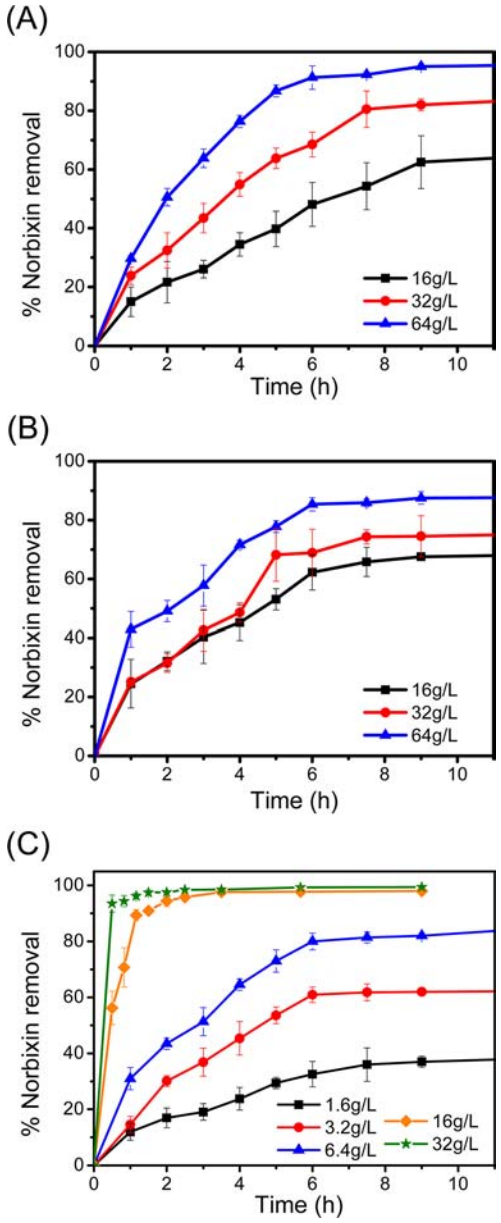

Figure 7. Kinetics of norbixin removal by different levels of CA (A), CB (B), and CNT (C) at pH 6.4 and 298 K. The data were calibrated by the degradation of norbixin. Error bars represent the range of duplicate samples.

Overall, the R^2 values were higher than 0.97 when the pseudo second order model was applied for all three adsorbents, and the estimated rate constant k_2 increased with the increasing dose of each adsorbent. This suggests that the rate constant k_2 can be used to compare adsorption properties of the three adsorbents. CB has a relatively higher k_2 than CA at three adsorbent levels due to its larger BET surface area. At an adsorbent level of 32 g/L, CNT has a much higher k_2 than CA and CB, while there is no big difference among the experimental q_e values of the three adsorbents, which is in accordance with their similar values of total volume of pores (Table 1).

For activated carbon, some micropore (<2 nm) openings may be blocked by the adsorbed norbixin molecular, while the functional groups of adsorptive sites located in the mesopores (2−50 nm) and macropores (>50 nm) are still accessible.[34] A large BET surface area is generally a requirement for a good adsorbent, but an adequate pore size is equally important.[35] Hsieh et al.[36] has demonstrated the importance of mesopores in enhancing the adsorption capacity of porous carbon, especially for large adsorbates. For CNT, the BET surface area is much smaller than CA and CB but the total microporosity ratio and pore width are much larger (Table 1), which may explain the higher adsorption rate of CNT.

Various mechanisms like external diffusion, boundary layer diffusion and intraparticle diffusion control the adsorption kinetics.[37] For porous adsorbents, the rate-limiting step is the intraparticle diffusion mechanism.[20] When fitting the data from CA and CB to the intraparticle diffusion model (eq 9), the regression of q_t versus $t^{1/2}$ is linear, with high R^2 (Table 3), and converges at the origin. Thus, the intraparticle diffusion appears to be the rate-limiting step for porous activated carbon (Table 1; Figure 1).[37] For CNT at higher dose, the lower R^2 value from the data fitting indicates that other steps such as external diffusion may be involved in the adsorption.[38] The deviation from the origin additionally suggests that the intraparticle diffusion is not the rate controlling mechanism for CNT.[39]

Thermodynamic Parameters of Adsorption. The energy involved in an ideal adsorption process is independent of the adsorption capacity.[40] However, adsorbents such as activated carbon have heterogeneous surfaces, and the energy associated with nonideal adsorption can affect the outcome.[40] In order to calculate thermodynamic parameters, the van't Hoff equation (eq 11) was applied using parameters derived from the Langmuir adsorption isotherms.[41]

$$\ln k_L = \frac{\Delta S}{R} - \frac{\Delta H}{RT} \quad (11)$$

dx.doi.org/10.1021/jf402537y | J. Agric. Food Chem. 2013, 61, 9230−9240

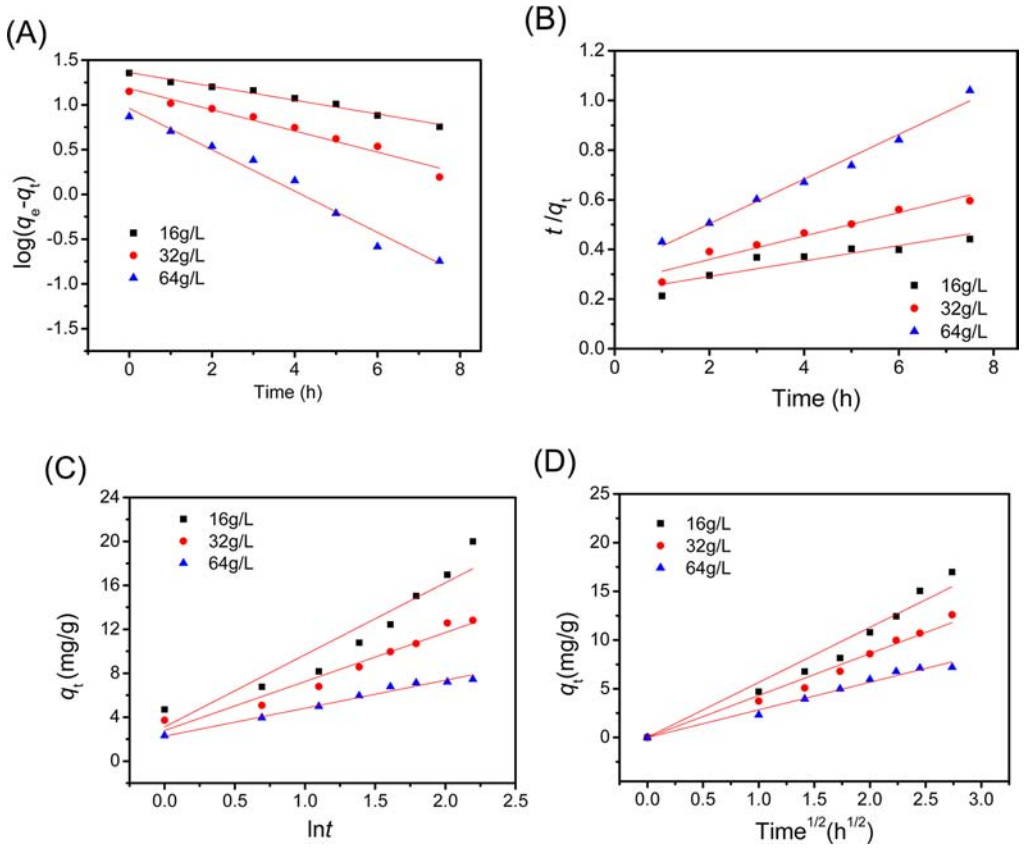

Figure 8. Kinetics of norbixin adsorbing onto three levels of CA at pH 6.4 and 298 K when fitting to (A) pseudo first order, (B) pseudo second order, (C) Elovich, and (D) intraparticle diffusion models. Data were calibrated by the degradation of norbixin.

where k_L is the Langmuir equilibrium constant (L/mol) in eq 3, R is the gas constant (8.314 J mol^{-1} K^{-1}), T is the absolute temperature (K), and ΔH and ΔS are the enthalpy and entropy changes associated with the adsorption, respectively.

The ΔH and ΔS determined from the slope and intercept of the van't Hoff plots are summarized in Table 4. The equilibrium constants were also used to determine the Gibbs free energy change (ΔG) by following equation:[42]

$$\Delta G = \Delta H - T\Delta S \quad (12)$$

The negative value of ΔH (Table 4) indicates the exothermic adsorption, showing that the adsorption of norbixin on all three adsorbents is favored at a lower temperature. The negative value of ΔG indicates that the adsorption is a spontaneous process. The exothermic adsorption lowers the system energy, with the ΔH estimated to be in the range of 8−65 kJ/mol when organic molecules adsorb from an aqueous solution onto activated carbon.[43]

Furthermore, smaller accessible pores are expected to have a more negative ΔH.[44] For the two activated carbon materials, the bigger micropore volume of CB than that of CA (Table 1) agrees this analysis (Table 4).[44] The positive ΔS value for CA shows the increased randomness of norbixin adsorbing on the solid surface. For CNT, the magnitude of ΔS is small, suggesting its insignificance in adsorption. Differences in ΔS can result from variations in adsorbate−adsorbent interactions and adsorbent structures,[45] which can impact equilibrium constants.[44] Although the negative ΔH of CB has a larger magnitude than that of CA, the two adsorbents show similar ΔG (similar equilibrium constant) because their ΔS contributions are opposite.

Effects of Ionic Strength on the Adsorption. Besides van der Waals interactions, hydrophobic interactions, $\pi-\pi$ interactions, solvent polarity, solution chemistry, and molecular dimensions are important in the adsorption.[46] For acid dyes, the molecule can be ionized to adsorb on charged adsorbent surface.[47] Norbixin has a highly hydrophobic carbon chain with two polar carboxylate head groups which facilitate both hydrophobic and electrostatic interactions with carbon surface. In order to study the significance of electrostatic interactions on the adsorption capacity, another batch of experiments was performed under room temperature at 0.1 and 0.5 M NaCl. Only pH 4.5, 6.4, and 9.0 were studied (Figure 9) to prevent the complications of norbixin precipitation at lower pH, as discussed previously. The norbixin removal efficiency of CA and CB decreased significantly with the increase in ionic strength. Conversely, the effects of ionic strength were pH-dependent for CNT, showing an increase in removal efficiency with an increase in NaCl concentration at the two lower pHs but the opposite at pH 9.0. The pH_{PZC} of CA and CB is 10.8 and 10.3, respectively (Figure 2), suggesting that the adsorbents are positively charged at the measuring pH 4.5−9.0. The pK_a for norbixin is about 4.8,[48] and thus a higher extent of dissociated norbixin is expected at a higher pH. The increased norbixin removal at a higher pH (Figure 9) emphasizes the significance of electrostatic attraction,[16] which is further supported by the lowered norbixin removal at higher NaCl concentrations (Figure 9) that weaken electrostatic attraction. For CNT, they are positively charged, while about one-half of the carboxylate groups of norbixin are dissociated at pH 4.5 (close to pK_a of norbixin, at pH 4.8), which coincided with the

dx.doi.org/10.1021/jf402537y | J. Agric. Food Chem. 2013, 61, 9230−9240

Table 3. Parameters Derived from Four Kinetics Models for Norbixin Adsorbing onto Adsorbents Used at Various Levels at pH 6.4 and 298 K

		CA (g/L)			CB (g/L)			CNT (g/L)				
kinetics model	parameters	16	32	64	16	32	64	1.6	3.2	6.4	16	32
	q_e (exptl, mg g^{-1})	22.66	14.14	7.59	21.56	11.72	7.65	134.38	98.75	67.95	30.50	15.55
pseudo 1st order	k_1 (h^{-1})	0.18	0.27	0.53	0.38	0.56	0.42	0.23	0.53	0.38	1.40	0.80
	q_e (mg g^{-1})	22.99	15.21	9.12	24.95	18.85	7.05	135.10	144.04	71.53	16.67	2.16
	R^2	0.9833	0.9676	0.9745	0.9430	0.8802	0.9619	0.9830	0.9294	0.9773	0.7508	0.7368
	AIC	−30.97	−18.68	−9.96	−8.34	4.30	−10.31	−26.44	−1.48	−16.18	20.87	12.57
pseudo 2nd order	k_2 (g mg^{-1} h^{-1})	0.0023	0.0058	0.0253	0.0074	0.0073	0.0528	0.00082	0.00087	0.0033	0.073	1.79
	q_e (mg g^{-1})	40.80	24.08	11.11	31.63	21.73	8.67	198.67	184.27	95.34	34.44	15.55
	h (mg g^{-1} h^{-1})	3.83	3.36	3.12	7.40	3.45	3.97	32.37	29.54	30.00	86.59	432.83
	R^2	0.9875	0.9926	0.9948	0.9822	0.9735	0.9757	0.9820	0.9926	0.9901	0.9825	0.9998
	AIC	20.16	11.08	0.74	25.94	20.76	10.81	53.27	45.08	40.02	33.26	−12.66
Elovich	α (mg g^{-1} h^{-1})	10.29	8.26	6.23	17.19	8.35	8.95	81.71	65.38	57.94	517.16	2.79×10^{3}
	β (g mg^{-1})	0.16	0.23	0.38	0.15	0.24	0.53	0.0263	0.0260	0.0471	0.19	0.52
	R^2	0.9175	0.9485	0.9863	0.9414	0.9107	0.9340	0.9285	0.9824	0.9664	0.7776	0.9743
	AIC	28.23	20.20	3.23	26.75	23.48	10.07	52.73	42.69	39.01	40.41	30.73
intraparticle diffusion	K_{dif} (mg g^{-1} $min^{-1/2}$)	5.65	4.31	2.84	7.47	4.19	2.51	39.55	35.64	24.47	12.53	5.23
	C (mg g^{-1})	3.18×10^{-12}	1.11×10^{-11}	6.29×10^{-7}	2.66×10^{-6}	7.11×10^{-10}	0.34	1.67×10^{-9}	1.05×10^{-8}	6.02×10^{-8}	8.51	6.97
	R^2	0.9588	0.9784	0.9808	0.9924	0.9647	0.9783	0.9824	0.9673	0.9905	0.7404	0.5086
	AIC	29.66	19.64	11.13	19.13	23.06	9.91	53.10	57.01	39.70	54.82	48.95

dx.doi.org/10.1021/jf402537y | J. Agric. Food Chem. 2013, 61, 9230−9240

Table 4. Thermodynamic Parameters for the Adsorption of Norbixin on Three Adsorbents at pH 6.4

	temp (K)	ΔG (kJ mol^{-1})	ΔH (kJ mol^{-1})	ΔS (J mol^{-1} K^{-1})
CA	298	−29.65	−27.50	7.22
	313	−29.76		
	328	−29.89		
CB	298	−29.94	−39.43	−31.84
	313	−29.46		
	328	−28.99		
CNT	298	−29.90	−29.65	0.83
	313	−29.91		
	328	−29.92		

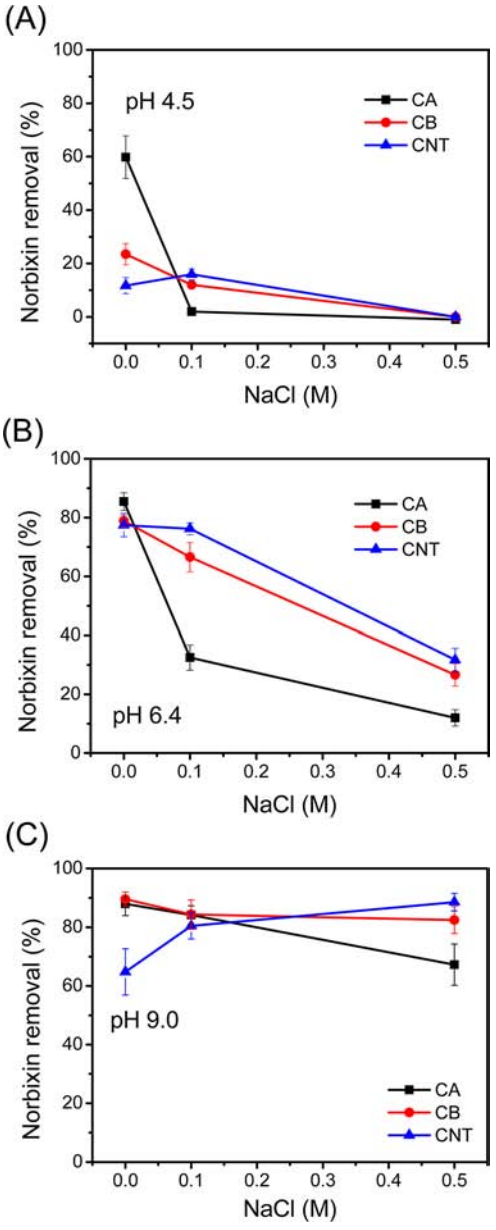

Figure 9. The effects of ionic strength on norbixin removal by three adsorbents at pH 4.5 (A), 6.4 (B), and 9.0 (C). The dosage of CA, CB, and CNT was 32, 32, and 3.2 g/L, respectively, and the incubation was 24 h at room temperature (23 °C). Error bars represent the range of duplicate samples.

small impact of ionic strength (Figure 9A). At pH 6.4, the adsorption capacity reaches the maximum for CNT, norbixin is dissociated to a greater extent than at pH 4.5, and an increase in NaCl concentration significantly reduced norbixin removal (Figure 9B). At pH 9.0 (above the pH_{PZC} of CNT), the overall electrostatic interactions between norbixin and CNT are repulsive, and the weakened repulsion at a higher NaCl concentration increased the norbixin adsorption/removal (Figure 9C). The results suggest that electrostatic forces are important for the adsorption of norbixin on the three adsorbents.

In summary, three carbonaceous agents showed great potential for the removal of norbixin from aqueous solutions, with the extent being a function of pH, adsorbent level, temperature, and ionic strength. At the whey pH and room temperature, the adsorption by CB was faster than CA due to its larger BET surface area, while CNT were more effective on reaching adsorption equilibria at a shorter time and a lower dose than both CA and CB due to its much higher microporosity ratio. The classic Freundlich and Langmuir models both fit the adsorption isotherm data well. The thermodynamic parameters estimated from adsorption isotherms demonstrated that the adsorption of norbixin on three adsorbents is exothermic, and the entropic contribution was a function of adsorbent structure. The adsorption kinetics for two activated carbon products followed both pseudo first and second order. But for CNT, it followed the pseudo first order at low doses while the pseudo second order at high doses. The kinetics data also stressed the significance of intraparticle diffusion for activated carbon. Finally, the effects of ionic strength on norbixin removal suggested the significant role of electrostatic attraction under the studied conditions. If the established adsorption parameters can be verified in cheese whey, these adsorbents may be applied in the dairy industry to decolorize cheese whey without applying bleaching agents.

AUTHOR INFORMATION

Corresponding Author

*Q. Zhong: Department of Food Science and Technology, The University of Tennessee, 2510 River Drive, Knoxville, TN 37996. Phone: (865) 974-6196. Fax: (865) 974-7332. E-mail: qzhong@utk.edu.

Funding

This work was sponsored by The University of Tennessee and Dairy Research Institute (Rosemont, IL).

Notes

The authors declare no competing financial interest.

REFERENCES

(1) Kang, E. J.; Campbell, R. E.; Bastian, E.; Drake, M. A. Invited review: Annatto usage and bleaching in dairy foods. *J. Dairy Sci.* **2010**, *93*, 3891−3901.

(2) Zhu, D.; Damodaran, S. Short communication: Annatto in Cheddar cheese-derived whey protein concentrate is primarily associated with milk fat globule membrane. *J. Dairy Sci.* **2012**, *95*, 614−617.

(3) Szweda, R.; Schmidt, K.; Zorn, H. Bleaching of colored whey and milk by a multiple-enzyme system. *Eur. Food Res. Technol.* **2013**, *237*, 377−384.

(4) Zhang, Y.; Zhong, Q. Probing the binding between norbixin and dairy proteins by spectroscopy methods. *Food Chem.* **2013**, *139*, 611−616.

(5) Pelekani, C.; Snoeyink, V. L. Competitive adsorption in natural water: role of activated carbon pore size. *Water Res.* **1999**, *33*, 1209−1219.
(6) Namasivayam, C.; Kavitha, D. Removal of Congo Red from water by adsorption onto activated carbon prepared from coir pith, an agricultural solid waste. *Dyes Pigments* **2002**, *54*, 47−58.
(7) Roy, G. M. *Activated Carbon Applications in the Food and Pharmaceutical Industries*; Technomic Publishing Company: Boca Raton, FL, 1995.
(8) Miyagi, A.; Nabetani, H.; Nakajima, M. Decolorization of Japanese soy sauce (shoyu) using adsorption. *J. Food Eng.* **2013**, *116*, 749−757.
(9) Upadhyayula, V. K. K.; Deng, S.; Mitchell, M. C.; Smith, G. B. Application of carbon nanotube technology for removal of contaminants in drinking water: A review. *Sci. Total Environ.* **2009**, *408*, 1−13.
(10) Akasaka, T.; Watari, F. Capture of bacteria by flexible carbon nanotubes. *Acta Biomater.* **2009**, *5*, 607−612.
(11) Rao, G. P.; Lu, C.; Su, F. Sorption of divalent metal ions from aqueous solution by carbon nanotubes: A review. *Sep. Purif. Technol.* **2007**, *58*, 224−231.
(12) Galano, A. Carbon nanotubes as free-radical scavengers. *J. Phys. Chem. C* **2008**, *112*, 8922−8927.
(13) Noh, J. S.; Schwarz, J. A. Effect of HNO3 treatment on the surface acidity of activated carbons. *Carbon* **1990**, *28*, 675−682.
(14) Parvin, K.; Aziz, M. G.; Yusof, Y. A.; Sarker, M. S. H.; Sill, H. P. Degradation kinetics of water-soluble annatto extract and sensory evaluation of annatto colored yoghurt. *J. Food Agric. Environ.* **2011**, *9*, 139−142.
(15) Scotter, M. J.; Wilson, L. A.; Appleton, G. P.; Castle, L. Analysis of annatto (Bixa orellana) food coloring formulations. 1. Determination of coloring components and colored thermal degradation products by high-performance liquid chromatography with photodiode array detection. *J. Agric. Food Chem.* **1998**, *46*, 1031−1038.
(16) Al-Degs, Y. S.; El-Barghouthi, M. I.; El-Sheikh, A. H.; Walker, G. M. Effect of solution pH, ionic strength, and temperature on adsorption behavior of reactive dyes on activated carbon. *Dyes Pigments* **2008**, *77*, 16−23.
(17) Benguella, B.; Benaissa, H. Cadmium removal from aqueous solutions by chitin: kinetic and equilibrium studies. *Water Res.* **2002**, *36*, 2463−2474.
(18) Chien, S. H.; Clayton, W. R. Application of Elovich equation to the kinetics of phosphate release and sorption in soils1. *Soil Sci. Soc. Am. J.* **1980**, *44*, 265−268.
(19) Allen, S. J.; McKay, G.; Khader, K. Y. H. Intraparticle diffusion of a basic dye during adsorption onto sphagnum peat. *Environ. Pollut.* **1989**, *56*, 39−50.
(20) El Nemr, A.; Abdelwahab, O.; El-Sikaily, A.; Khaled, A. Removal of direct blue-86 from aqueous solution by new activated carbon developed from orange peel. *J. Hazard. Mater.* **2009**, *161*, 102−110.
(21) Ho; Ho, Y. S.; McKay; McKay, G.; Wase; Wase, D. A. J.; Forster; Forster, C. F. Study of the sorption of divalent metal ions on to peat. *Adsorpt. Sci. Technol.* **2000**, *18*, 639−650.
(22) Burnham, K. P.; Anderson, D. R. *Model Selection and Multi-Model Inference: A Practical Information-Theoretic Approach*; Springer: New York, NY, 2002.
(23) Scherdel, C.; Reichenauer, G.; Wiener, M. Relationship between pore volumes and surface areas derived from the evaluation of N2-sorption data by DR-, BET- and t-plot. *Microporous Mesoporous Mater.* **2010**, *132*, 572−575.
(24) Li, L.; Li, X.; Lee, J.-Y.; Keener, T. C.; Liu, Z.; Yao, X. The Effect of surface properties in activated carbon on mercury adsorption. *Ind. Eng. Chem. Res.* **2012**, *51*, 9136−9144.
(25) Kobya, M.; Demirbas, E.; Senturk, E.; Ince, M. Adsorption of heavy metal ions from aqueous solutions by activated carbon prepared from apricot stone. *Bioresour. Technol.* **2005**, *96*, 1518−1521.
(26) Al-Degs, Y.; Khraisheh, M. A. M.; Allen, S. J.; Ahmad, M. N. Effect of carbon surface chemistry on the removal of reactive dyes from textile effluent. *Water Res.* **2000**, *34*, 927−935.
(27) El Qada, E. N.; Allen, S. J.; Walker, G. M. Adsorption of methylene blue onto activated carbon produced from steam activated bituminous coal: A study of equilibrium adsorption isotherm. *Chem. Eng. J.* **2006**, *124*, 103−110.
(28) Shumaker, E. K.; Wendorff, W. L. Factors affecting pink discoloration in annatto-colored pasteurized process cheese. *J. Food Sci.* **1998**, *63*, 828−831.
(29) Damodaran, S. Zinc-induced precipitation of milk fat globule membranes: A simple method for the preparation of fat-free whey protein isolate. *J. Agric. Food Chem.* **2010**, *58*, 11052−11057.
(30) Giles, C.; MacEwan, T.; Nakhwa, S.; Smith, D. 786. Studies in adsorption. Part XI. A system of classification of solution adsorption isotherms, and its use in diagnosis of adsorption mechanisms and in measurement of specific surface areas of solids. *J. Chem. Soc.* **1960**, 3973−3993.
(31) Reddad, Z.; Gerente, C.; Andres, Y.; Le Cloirec, P. Adsorption of several metal ions onto a low-cost biosorbent: Kinetic and equilibrium studies. *Environ. Sci. Technol.* **2002**, *36*, 2067−2073.
(32) Ho, Y. S.; McKay, G. Sorption of dye from aqueous solution by peat. *Chem. Eng. J.* **1998**, *70*, 115−124.
(33) Rudzinski, W.; Plazinski, W. Studies of the kinetics of solute adsorption at solid/solution interfaces: On the possibility of distinguishing between the diffusional and the surface reaction kinetic models by studying the pseudo-first-order kinetics. *J. Phys. Chem. C* **2007**, *111*, 15100−15110.
(34) Kadirvelu, K.; Faur-Brasquet, C.; Cloirec, P. L. Removal of Cu(II), Pb(II), and Ni(II) by adsorption onto activated carbon cloths. *Langmuir* **2000**, *16*, 8404−8409.
(35) Li, Y.-H.; Wang, S.; Luan, Z.; Ding, J.; Xu, C.; Wu, D. Adsorption of cadmium(II) from aqueous solution by surface oxidized carbon nanotubes. *Carbon* **2003**, *41*, 1057−1062.
(36) Hsieh, C.-T.; Teng, H. Influence of mesopore volume and adsorbate size on adsorption capacities of activated carbons in aqueous solutions. *Carbon* **2000**, *38*, 863−869.
(37) Wu, C. H. Adsorption of reactive dye onto carbon nanotubes: Equilibrium, kinetics and thermodynamics. *J. Hazard. Mater.* **2007**, *144*, 93−100.
(38) Figaro, S.; Avril, J. P.; Brouers, F.; Ouensanga, A.; Gaspard, S. Adsorption studies of molasse's wastewaters on activated carbon: Modelling with a new fractal kinetic equation and evaluation of kinetic models. *J. Hazard. Mater.* **2009**, *161*, 649−656.
(39) Tofighy, M. A.; Mohammadi, T. Adsorption of divalent heavy metal ions from water using carbon nanotube sheets. *J. Hazard. Mater.* **2011**, *185*, 140−147.
(40) Himeno, S.; Komatsu, T.; Fujita, S. High-pressure adsorption equilibria of methane and carbon dioxide on several activated carbons. *J. Chem. Eng. Data* **2005**, *50*, 369−376.
(41) Fan, T.; Liu, Y.; Feng, B.; Zeng, G.; Yang, C.; Zhou, M.; Zhou, H.; Tan, Z.; Wang, X. Biosorption of cadmium(II), zinc(II) and lead(II) by *Penicillium simplicissimum*: Isotherms, kinetics and thermodynamics. *J. Hazard. Mater.* **2008**, *160*, 655−661.
(42) Hu, Y.-J.; Liu, Y.; Wang, J.-B.; Xiao, X.-H.; Qu, S.-S. Study of the interaction between monoammonium glycyrrhizinate and bovine serum albumin. *J. Pharm. Biomed. Anal.* **2004**, *36*, 915−919.
(43) Mattson, J. S.; Mark, H. B. *Activated Carbon: Surface Chemistry and Adsorption from Solution*; Marcel Dekker: New York, NY, 1971.
(44) Everett, D. H.; Powl, J. C. Adsorption in slit-like and cylindrical micropores in the henry's law region. A model for the microporosity of carbons. *J. Chem. Soc., Faraday Trans. 1* **1976**, *72*, 619−636.
(45) Drago, R. S.; Webster, C. E.; McGilvray, J. M. A multiple-process equilibrium analysis of silica gel and HZSM-5. *J. Am. Chem. Soc.* **1998**, *120*, 538−547.
(46) Liu, Q.-S.; Zheng, T.; Wang, P.; Jiang, J.-P.; Li, N. Adsorption isotherm, kinetic and mechanism studies of some substituted phenols on activated carbon fibers. *Chem. Eng. J.* **2010**, *157*, 348−356.
(47) Mohamed, M. M. Acid dye removal: comparison of surfactant-modified mesoporous FSM-16 with activated carbon derived from rice husk. *J. Colloid Interface Sci.* **2004**, *272*, 28−34.

(48) Sharma, P.; Bora, M. M.; Borthakur, S.; Rao, P. G.; Dutta, N. N. Separation of norbixin from Bixa orellana seed raw dye by Aliquat-336. *Environ. Prog. Sustainable Energy* **2012**, *32* (1), 134−138.